

Mechanical Behavior of Single-Layer Two-Way Grid Cylindrical Latticed Shell with Out-of-Plane Tension Members

Zhang Zhonghao^{1,2}, Ma Huihuan^{3,*}, Fujimoto Masumi⁴ and Fu Qiang¹

¹School of Water Conservancy and Civil Engineering, Northeast Agricultural University, Harbin, 150030, China

²School of Civil Engineering, Harbin Institute of Technology, Harbin, 150090, China

³School of Civil Engineering, Harbin Institute of Technology, Harbin, China, 150090, +8618345141582,

⁴Osaka City University, Osaka, 558-8585, Japan

Abstract: Single layer two-way grid shell with in-plane and out-of-plane tension members is a new type of single-layer latticed shell roof. This study treats the effects of tension member installation on the buckling load and strength of a single layer two-way grid cylindrical shell roof by the numerical method. The tension members are installed to stiffen the rigidity of a single layer two-way grid shell roof and improve its stability behavior. Tension member installation and placement pattern is focused as both diagonal members of two-way grids and out-of-plane stiffened members in a cylindrical surface. The diagonal member and the out-of-plane member are used to increase the in-plane and the out-of-plane rigidity of a single layer two-way grid shell, respectively. The tension member placement pattern, the load distribution patterns, the initial imperfections and the initial axial force are considered for the numerical calculation parameters. It is confirmed by the numerical analysis that the tension members in out-of-plane and diagonals caused the increase in the buckling and strength of two-way grid shell.

Keywords: Buckling load, placement pattern, single layer two-way grid shell, strength, tension member.

1. INTRODUCTION

Among the long-span spatial structures, the single layer grid shell has many advantages compared to the multi-layer grid shell, because of the characteristics of being light-duty and economically produced. Single layer grid shell has a high rigidity relative to weight. Therefore, the single layer grid shells are used for the public building and the gymnasium.

The reticulation patterns of single layer grid shell are triangle, two-way grid, and hexagonal mesh, etc. The in-plane rigidity of two-way grid is lower than that of triangular mesh. But the two-way grid is superior in aesthetics and material efficiency. To make up for the defect of two-way grid and to maintain aesthetics, the single layer two-way grid shells stiffened with tension member are proposed [1-3]. The buckling experiment of single layer two-way grid dome with PC bars as diagonal members was made to show that the rigidity and the buckling load of these domes are increased by the effect of the initial axial force of PC bars [4, 5]. It is shown that the buckling load of a single layer two-way grid shell with the

diagonal tension member installation is larger than that of a single layer two-way grid shell without the tension member [6, 7]. The buckling strength estimated formula is aimed at two-way single-layer lattice domes with diagonal braces [8].

In recent years, the construction of buildings with tension members are increasing and two-way grid shell with out-of-plane tension members appeared. Hamburg City History Museum is a two-way grid shell with glass exterior and stiffened with tension members in the arch plane [9]. The examples of building with tension members are listed and two-way grid is shown through them [10, 11]. To increase out-of-plane stiffness of single layer latticed dome, suspended dome with strut and out-of-plane tension members are proposed and the effects on buckling load is examined by the experimental study [12].

However, there are few researches on the parameter of tension member in out-of-plane installation. This paper studies single layer two-way grid cylindrical shell roof with tension members in out-of-plane and diagonal members. The effect of tension members on buckling load and strength of a single layer two-way grid shell roof are investigated. To improve the rigidity of in-plane-direction shear stiffness and out-of-plane stiffness, the effect of tension member installation on buckling load and strength are examined by linear bifurcation buckling analysis and

*Address correspondence to this author at the School of Civil Engineering, Harbin Institute of Technology, Harbin, China, 150090; Tel: +8618345141582; E-mail: mahuihuan@hit.edu.cn

nonlinear analysis. The number of units, grid member length, load distribution, initial imperfection and the initial axial force of tension member are given as analytical parameters and the effectiveness of out-of-plane and diagonal tension members is discussed by this study.

2. ANALYTICAL OBJECT

2.1. Analytical Model

The analytical model is a single layer two-way grid cylindrical shell roof with tension members in out-of-plane and diagonals. Fig. (1) shows the overall view of a single layer two-way grid cylindrical shell roof (unit number n=6). In this figure, X, Y, and Z are cylindrical coordinates. *u*, *v* and *w* are displacements corresponding to X, Y, and Z, respectively. The configuration parameters of the shell are as follows. *L_x* is generatrix direction length, *L_y* is span length, *l* is grid member length, $R=l/(2\sin(\alpha/n))$ is the radius of curvature and α is the half open angle in arch direction. The half open angle subtended by arch is 30°. Table 1 shows the configuration parameters of single layer two-way grid cylindrical shell.

Fig.(2-a) shows the types of the cylindrical shell roof with tension members in out-of-plane (T5, T6, T8, T9, T11) called T series. T5 is stiffened with tension members and struts. The length of strut in T5 is two times larger than the rise formed by 2x2 units as shown in Fig. (3). Fig.(2-b) shows the types of the two-way grid shell with tension members in out-of-plane and diagonals (TD, TD6, TD8, TD9, TD11) called TD series. TD6 and TD8 are stiffened with tension members and vertical member in out-of-plane. Fig. (3). shows the side view of types. The vertical members in the central position of T6 and T8 are tension members, and the vertical members in the central position of TD6 and TD8 are struts. The length of vertical member is one half of the rise of the two-way grid shell.

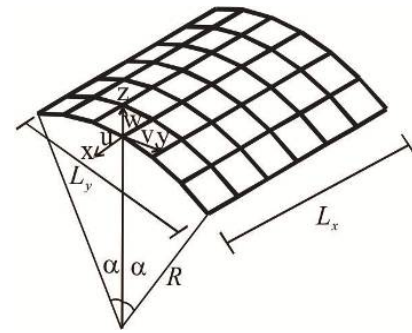


Fig. (1). Overall view of single layer two-way grid cylindrical shell

The properties of members are shown in Table 2. The two-way grid member is a steel pipe (φ165.2x7) and the tension member is a PC bar (φ20). The strut is steel bar and the slenderness is 200 expect for T5.

2.2. Supporting Condition and Load Distribution

The peripheral nodes in the gable are roller-supported in longitudinal direction. The peripheral nodes in the longitudinal direction are pin-supported. The applied load is the snow load. The load distribution is expressed with $\beta=q_R/q_L$ as shown in Fig. (4). $\beta=1.0$ (full), 0.9, 0.5, 0.0 (half) are used. The distributed load for action on node is concentrated load.

2.3. Initial Imperfections

The two-way grid shells with and without initial imperfection are called perfect system and imperfect system, respectively. Initial imperfection of geometry is assumed as one buckling mode in normal direction as shown in Eq. (1).

$$w = \mp w_{mm} \sin \frac{m_x \pi x}{L_x} \sin \frac{n_y \pi (y + R\alpha)}{2R\alpha} \tag{1}$$

Table 1. Configuration of two-way grid cylindrical shell.

<i>l</i> (cm)	n	<i>L_x</i> (cm)	<i>L_y</i> (cm)	<i>R</i> (cm)
300	4	1200	1149	1149
	6	1800	1721	1721
	8	2400	2293	2293
500	4	2000	1915	1915
	6	3000	2868	2868
	8	4000	3822	3822

Table 2. Property of grid member.

Member	Diameter (cm)	Thickness (cm)	<i>A</i> (cm ²)	<i>Z_p</i> (cm ³)	<i>I</i> (cm ⁴)	<i>E</i> (kN/mm ²)	v	σ_i (N/mm ²)
grid	16.52	0.7	34.79	175.3	1091	205.8	0.3	235
tension	2.0	–	3.14	1.33	0.79	205.8	0.3	1300
strut (T5)	7.63	0.4	9.09	88.35	59.5	205.8	0.3	235

w is displacement in normal direction of cylindrical coordinate system, w_{mm} is the imperfection amplitude in normal direction. m_x is the half wave number of buckling mode in longitudinal direction, n_y is the half wave number of buckling mode in arch direction. In this study, $m_x=1, n_y=1, 2$ and 3. The ratios of imperfection amplitude to the span are 1/1000 and 1/500. Initial imperfection is considered on the type of tension member arrangement as shown in Fig.(2).

3. ANALYTICAL METHOD

The member incremental elasticity rigidity matrix is based on the tangential rigidity matrix using stability function. Tension members are treated as the truss members in linear buckling analysis. In nonlinear analysis, tension members have rigidity in tension deformation of the elastic range. The yield and deformation after the yield of the tension member and the initial yield of grid member are considered as the material non-linearity. The incremental

displacement method and the arch length increment method are adopted in the calculation of equilibrium path [5].

4. ANALYTICAL RESULT

4.1. Linear Buckling Load

4.1.1. Effect of Tension Member Installation on Buckling Load

The buckling load P_{cr} denotes the gravity load of the center node. Table 3, Fig. (5) and Fig. (6) show the buckling load of each type when $\beta = 1.0$. In addition, the buckling load and strength of each type is $2/(1+\beta)$ times as the concentrated load acts on the central node.

In case of $l=500$, as for the buckling load of T series, T5 is higher than that of other types in T series. Compared to T9, T8 and T11 are in a range of 81%~84% ($n=4$), 60%~68% ($n=6$), and 66%~76% ($n=8$), respectively. As for the buckling load of TD series, TD8 is higher than the other

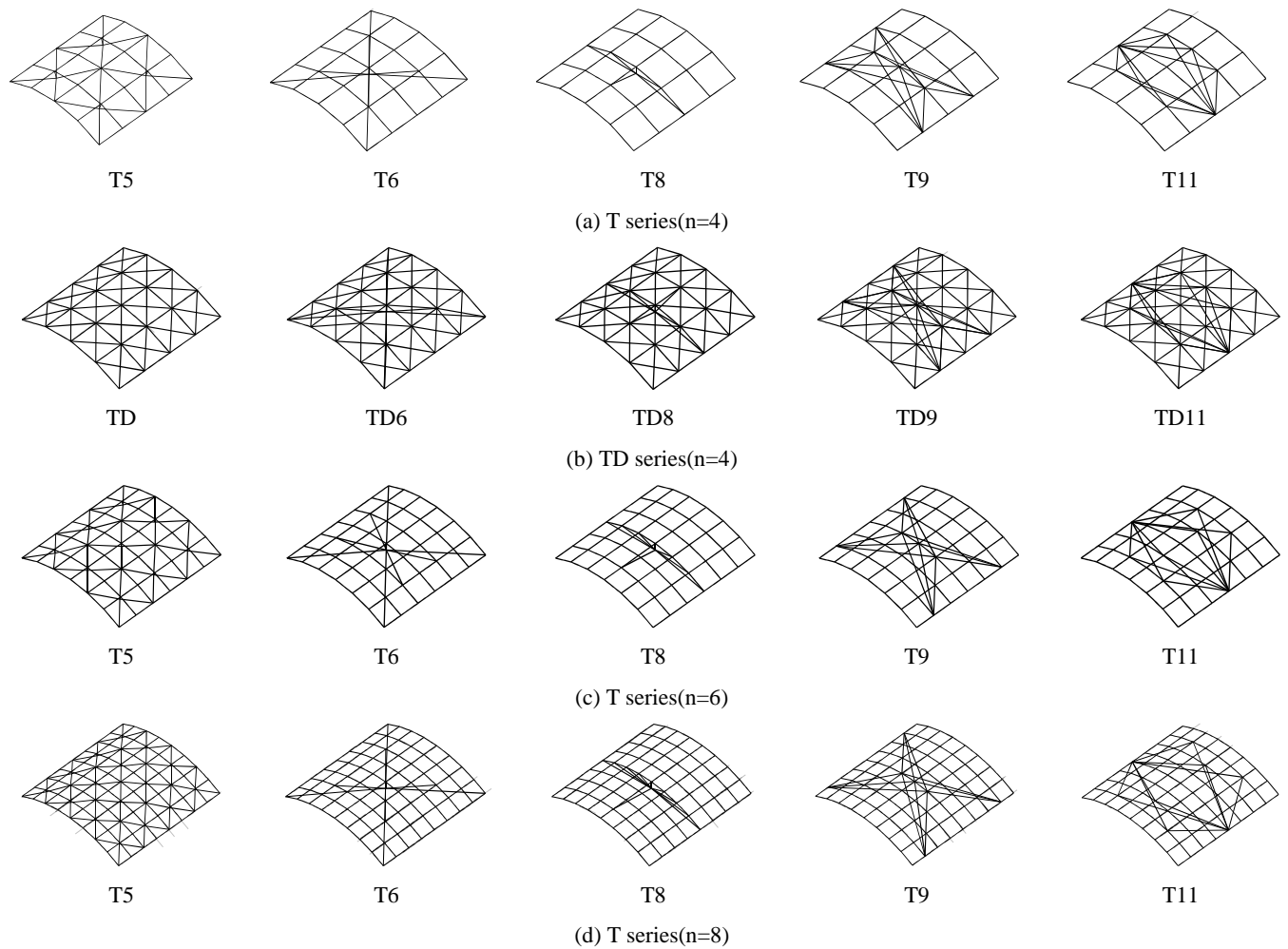


Fig. (2). Type of tension member arrangement

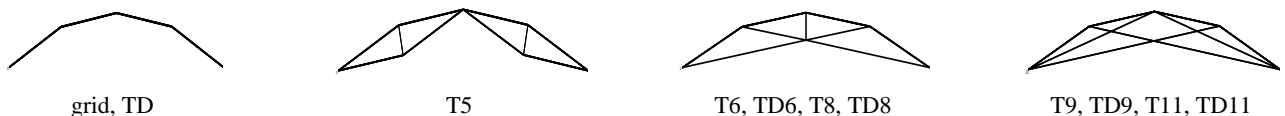


Fig. (3). Type of tension member arrangement (n=4)

Table 3. Buckling load of each type (kN).

<i>l</i> (cm)	<i>n</i>	Grid	T5	T6	T8	T9	T11	TD	TD6	TD8	TD9	TD11
300	4	254.2	535.7	347.8	491.6	594.2	489.9	445.7	547.2	360.7	644.6	571.2
	6	79.5	210.4	119.8	191.8	177.7	182.4	150.7	211.2	246.9	201.2	203.9
	8	35.6	83.5	59.2	92.2	81.8	65.8	69.5	94.8	128.1	100.1	86.3
500	4	91.2	260.9	167.1	216.9	218.5	211.6	186.5	278.7	278.4	281.6	254.0
	6	28.6	122.7	56.2	74.2	74.1	83.8	65.2	85.5	119.0	103.5	93.0
	8	12.8	43.7	29.0	33.2	33.3	29.0	33.2	36.5	58.5	48.1	37.7



Fig.(4). Load distribution

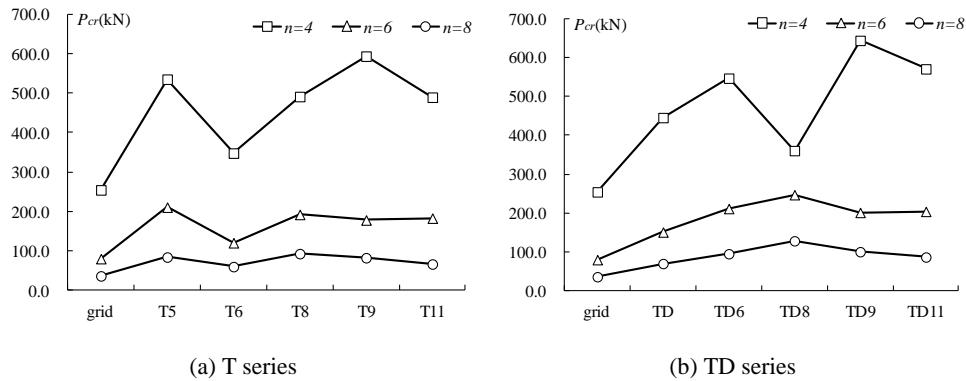


Fig. (5). Buckling load (*l*=300)

types, TD9, TD11, and TD6 are in a range of 82%~87%, 64%~78%, 62%~72% respectively, compared to TD8.

In case of *l*=300, as for the buckling load of T series, T5 is higher than that of other types expect for T9 of *n*=4 and T8 of *n*=8. T11, T8, and T9 show the value of 80%~90% compared to T5 and T6 is the minimum. As for the buckling load of TD series, TD8 is the maximum expect for *n*=4, and compared to TD8, other types show the value of 81%~86% when *n*=6 and 67%~78% when *n*=8. The buckling load of TD8 is lower than that of other types because of the strut member buckling when *n*=4.

4.1.2. Relation between Buckling Load and Radius of Curvature

Fig. (7) shows the relation between buckling load and radius of curvature when $\beta=1.0$. Fig. (8) shows the ratio of buckling load (*n*=6 and *n*=8) to buckling load (*n*=4) when $\beta=1.0$. As for the buckling load of the T series, *n*=6 decreases 30%~47% and *n*=8 decreases 13%~19% compared to *n*=4. As for the buckling load of TD series, *n*=6 decreases 31%~39%, *n*=8 decreases 13%~18% compare to *n*=4. As for the buckling load of TD8, in case of *l*=500, *n*=6 decreases 43%, *n*=8 decreases 36%, in case of *l*=300, *n*=6

decreases 68%, *n*=8 decreases 21%, respectively compared to *n*=4.

The reducing rate due to unit increasing is examined by the linear buckling load formula of pin supported arch. Linear buckling load is shown in Eq.(3) that is obtained by Eq.(2) without considering the difference in the direction of the load.

$$q_{cr}^{lin} = \frac{\pi^2 EI_y}{R^3 \phi_0^2} \tag{2}$$

$$p_{cr}^{lin} = q_{cr}^{lin} l = q_{cr}^{lin} \frac{2R\phi_0}{n} = \frac{2\pi^2 EI_y}{nR^2 \phi_0} \tag{3}$$

Here, *E* is elastic modulus, *R* is radius of curvature, *I_y* is second moment of area of grid member, ϕ_0 is the half open angle, *l* is the length of the grid, *n* is number of units. The ratio of buckling load (*n*₁) to buckling load (*n*₂) is shown in Eq. (4).

$$\frac{p_{cr}^{lin}(n_1)}{p_{cr}^{lin}(n_2)} = \frac{n_2 R_{n_2}^2}{n_1 R_{n_1}^2} \tag{4}$$

It is shown that the buckling load of *n*=6 and *n*=8 have decreased 30% and 13% respectively compared to that of

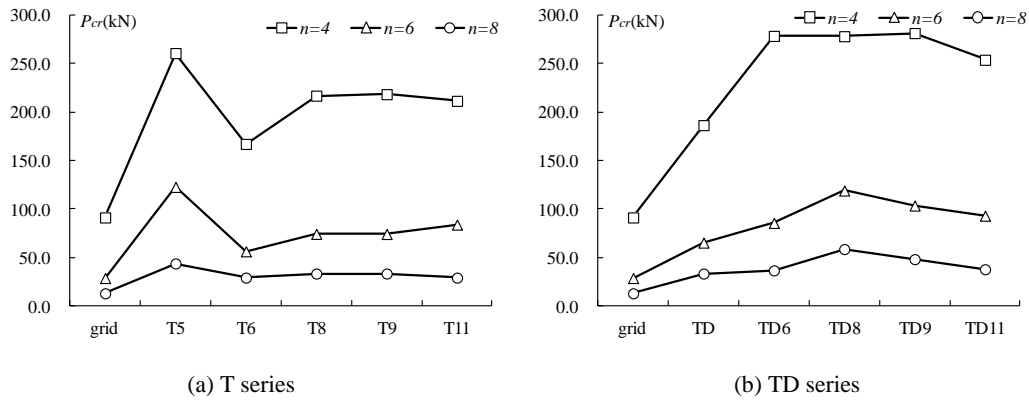


Fig. (6). Buckling load ($l=500$)

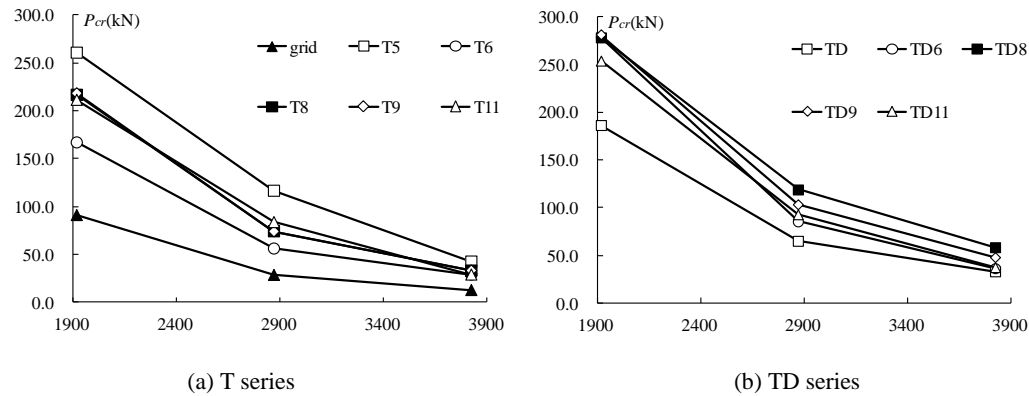


Fig. (7). Relation between buckling load and radius of curvature ($l=500$)

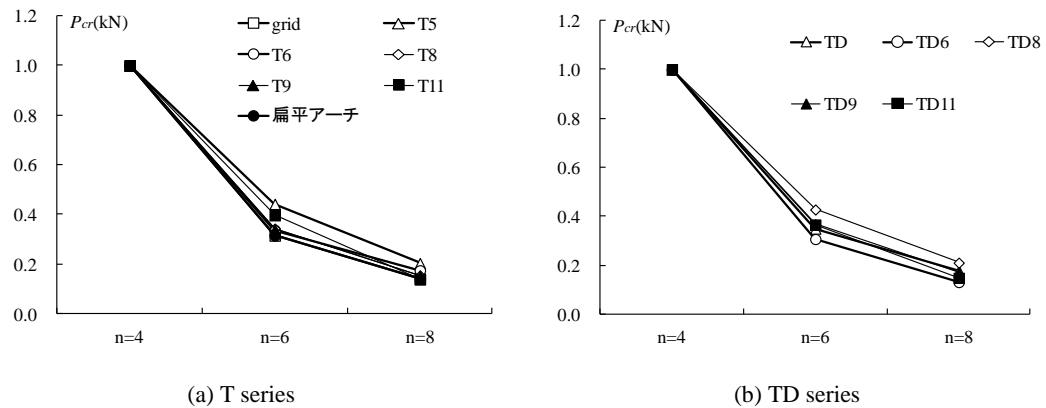


Fig. (8). Reducing rate ($l=500$)

$n=4$, once the value in Table (1) is substituted in Eq. (4). As shown in Fig (8) it corresponds with the analytical result of two-way grid shell roof.

4.1.3. Effect of Asymmetry Load

Fig. (9) shows the buckling load of each type and that β as a variable when $n=6$ and $l=300$. Compared to $\beta=1.0$, the buckling load of roofs with $\beta=0.9$, $\beta=0.5$ and $\beta=0.0$ increases 106%~109%, 139%~163%, and 213%~311%, respectively. As for the $n=6$, $l=300$, the buckling load of TD8 when $\beta=0.5$ and $\beta=0.0$ are lower compared to $\beta=1.0$ because of strut member buckling.

4.1.4. Buckling Mode and Axial Force

Fig. (10) shows the buckling mode and Table (4) shows the half wave number of buckling mode in center arch. As for the half wave number of buckling mode in center arch direction, T series are nearly 2~3, TD series are nearly 2~4 and TD series tend to be more than T series.

The half wave number of buckling mode in arch direction increases when grid member length l is increased and when $\beta=1.0$. Furthermore, the half wave number of buckling mode in arch direction decreases when β becomes small and is almost twice when $\beta=0.0$. As shown in Fig. (10), the half wave number of buckling mode in the longitudinal direction

is almost 1 except for T8 and TD8. The circle ○ in Table 4 show the strut member buckling.

4.2. Nonlinear Buckling Load and Strength

4.2.1. Perfect System

Table 5, Fig.(11) shows the strength of each type in perfect system when β is 1.0. In case of $l=500$, as for the strength of T series, T9 in $n=4$ is the maximum. The strength of T6, T11 and T8 show 84%~95% the value of T9. T9 and T11 are almost the same as two-way grid shell when $n=6$.

Strength of T8 is the maximum and T9 is almost the same as two-way grid shell when $n=8$. In case of TD series, strength of TD8 is the maximum expect for $n=4$, and increased 131%~198% compared to TD. Strength of TD6 is 75%~81% of TD8 and strength of TD9 and TD11 are almost the same as TD. When $n=4$, TD6 and TD9 show the almost the same value of TD8.

In case of $l=300$, strength of T series are almost the same when $n=4$ and the effects of tension members has not appeared. In case of TD series, strength of TD8 is the maximum; strength of TD6 shows the 86%~99% the value

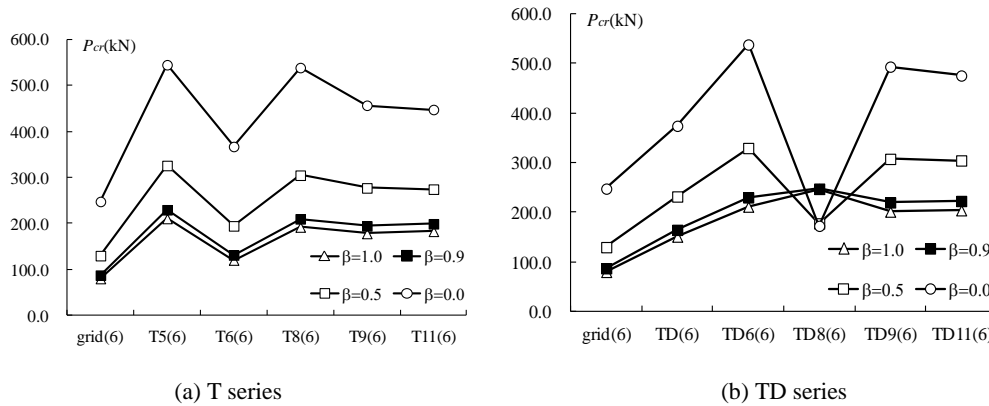


Fig. (9). Effect of the asymmetry load ($n=6, l=300$)

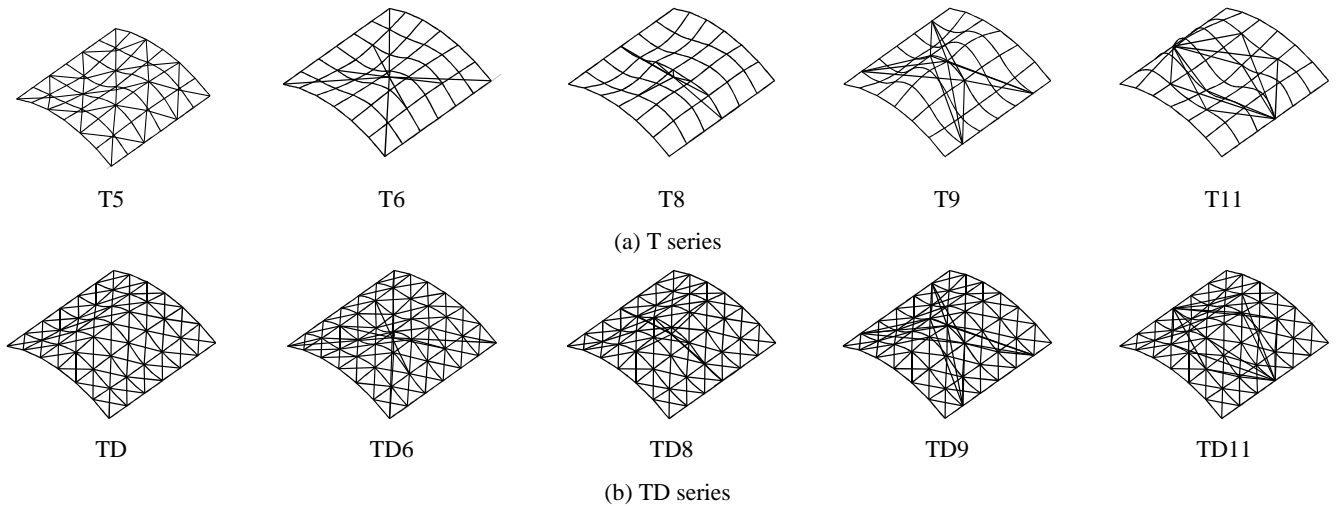


Fig. (10). Buckling mode ($n=6, l=300$)

Table 4. The half wave number ($\beta=1.0$).

l (cm)	n	Grid	T5	T6	T8	T9	T11	TD	TD6	TD8	TD9	TD11
300	4	2	2	2	2	3	2	2	○	○	3	3
	6	2	2	2	2	3	3	3	4○	3	3	3
	8	2	3	2	3	3	2	3	4	3	3	3
500	4	2	3	2	2	2	3	3	4	4	3	3
	6	2	4	3	2	3	4	3	4	4	3	4
	8	2	3	2	3	3	2	3	4	4	4	4

of TD8 and strength of TD9 and TD11 are almost the same as TD.

To examine the effect of diagonal tension members, $\beta=1.0$ as an example, making a comparison between strength of T series and that of TD series.

In case of $n=4$, $l=300$, TD8 increases 106% in comparison with T8. Compared to T6, TD6 increases 124%, 142% and 168% in case of $n=4$, $l=500$, $n=8$, $l=300$ and $n=8$, $l=500$, respectively. Compared to T9 and T11, TD9 and TD11 show 112% and 146% the value in case of $n=6$, $l=300$ and $n=6$, $l=500$, respectively. The strength of TD series increases 110%~170% compared to T series except for TD6 with $n=6$ and TD9, TD11 with $n=4$.

In addition, the effect of diagonal tension member on the strength becomes larger when the length of grid member grows.

4.2.2. Imperfection System

The strength (imperfection is considered) are defined by the minimum value of 12 kinds of imperfections. The ratio of strength in perfect system to the strength in imperfect system is examined by a reduction coefficient. Fig. (12) and Fig. (13) show the strength ratio when $n=6$.

As for the reduction coefficient, T9, TD6, TD8 and TD9 are in the 0.59~0.61 range in case of $n=4$, $l=500$ when $\beta=1.0$. In case of $n=6$, $l=500$, reduction coefficient of T8

Table 5. Strength of each type when β is 1.0 (kN).

l (cm)	n	Grid	T5	T6	T8	T9	T11	TD	TD6	TD8	TD9	TD11
300	4	192.7	193.4	192.7	192.8	193.9	192.6	193.4	202.6	204.7	194.6	193.4
	6	79.5	96.3	109.2	104.6	79.7	79.5	88.8	107.5	116.0	89.1	89.0
	8	36.0	47.9	43.0	56.8	36.0	42.0	44.4	61.0	71.1	44.7	45.1
500	4	90.9	112.0	124.4	141.0	148.4	129.2	122.8	154.8	153.1	152.7	131.9
	6	28.8	49.5	53.5	52.1	28.9	28.9	42.0	47.0	63.0	42.1	42.1
	8	13.0	22.7	18.9	28.4	13.1	17.7	19.7	31.7	39.1	19.9	20.7

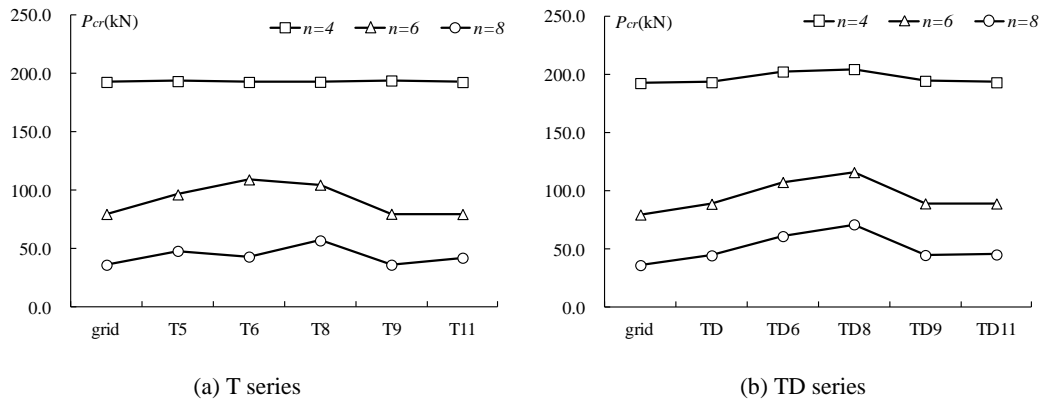


Fig. (11). Strength in perfect system ($\beta=1.0$, $l=300$)

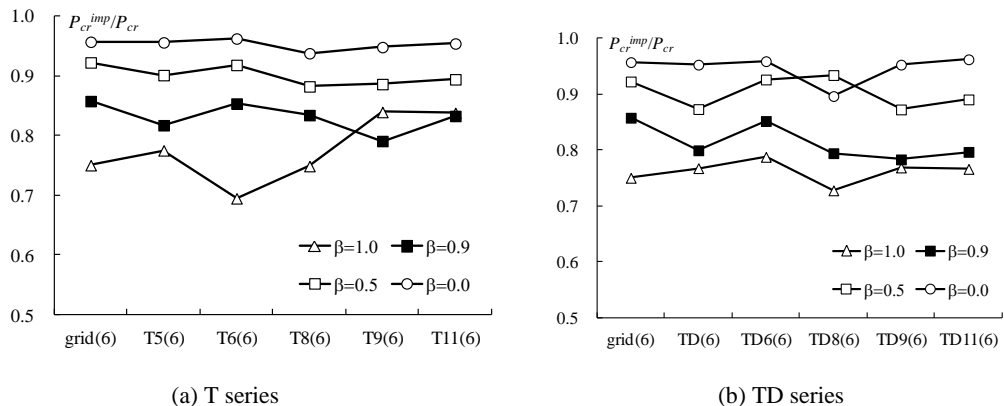


Fig. (12). Strength ratio ($n=6$, $l=300$)

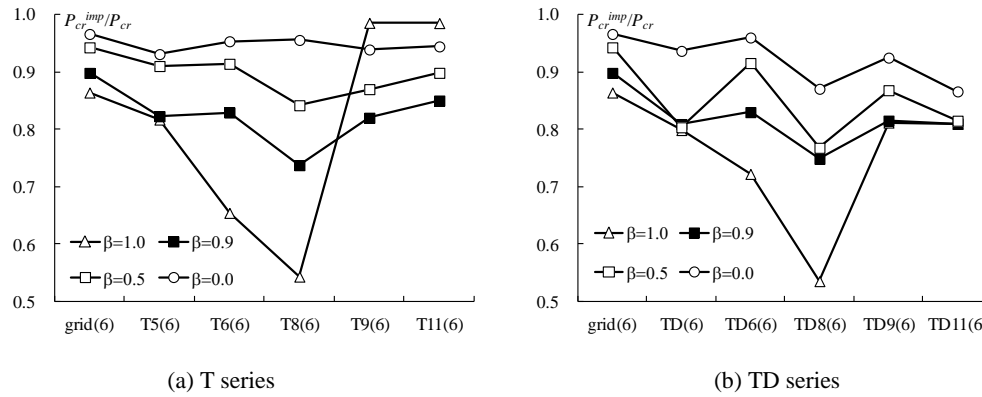


Fig. (13). Strength ratio ($n=6, l=500$)

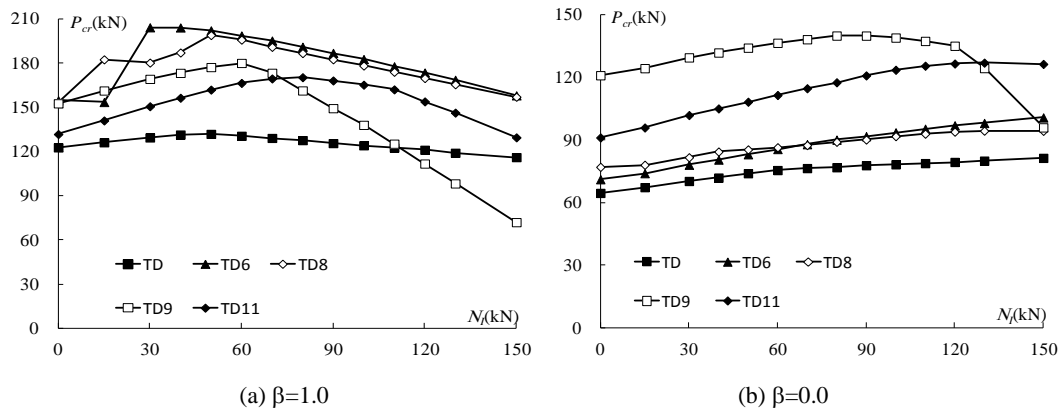


Fig. (14). The relation of strength and initial axial force ($n=4, l=500$)

and TD8 are the minimum and the value is 0.54 when $\beta=1.0$ and $n=8$, T8 and TD8 are 0.45 and 0.67, respectively. The reduction coefficient tends to increase when β decrease.

4.2.3. Effect of Initial Axial Force of Tension Member

The relation of strength and initial axial force is shown in Fig. (14). The strength of each type increases when the axial force N_l is increased and after the maximum, the strength applied decreases.

In case of $\beta=1.0$, compared with the situation $N_l=0$, the maximum strength due to initial axial force of TD, TD6, TD8, TD9 and TD11 increase 107%, 132%, 130%, 118% and 129%, respectively. In case of $\beta=0.5$, compared with the situation $N_l=0$, the maximum strength due to initial axial force of TD, TD6, TD8, TD9 and TD11 increase 123%, 134%, 122%, 108% and 131%, respectively.

The strength of TD9 rapidly reduces when the initial axial force exceeds a certain value. As a result of the axial force, of the member in the center arch, increase rapidly accompanied with the strength decrease as the member reaches initial yield.

5. CONCLUSION

This study focused on the tension member installation and examined the effect of tension member on buckling load and strength of single layer two-way grid shell, taking account of the units of grid, load distribution, initial

imperfection and the initial axial force. The effect of diagonal and out-of-plane tension member installation is discussed by numerical analysis. Acquired conclusions are given below.

(1) The buckling load of T5, that the tension member stiffened through the strut in each 2x2 unit, is higher than that of other types and 2.1 times larger than that of single layer two-way grid shell in case of T series. The buckling load of TD8 is higher than that of other types expect for $n=4, l=300$, and 3.1 times larger than that of a single layer two-way grid shell in case of TD series. The buckling load has a tendency to increase when β decreases.

(2) The strength of each type in T series increased due to the out-of-plane tension member installed in spite of the unit and the load asymmetry expect for $n=4, l=300$ when β is 1.0. In case of symmetrical load, the buckling load of TD8 is higher than that of other types and increased 106%~301% compared to two-way grid shell in TD series. In case of asymmetrical load, the effect of out-of-plane tension member installation appeared when $n=4$. The effect of out-of-plane tension member of TD9 and TD11 also appeared in $n=6$ and $n=8$ when the load asymmetry become evident.

(3) The reducing coefficient, by initial imperfection, is in a range of 0.45~0.67 when $\beta=1.0$ and in a range of 0.83~0.99 when $\beta=0.0$. The reducing coefficient is close to 1.0 when β decreases.

(4) The increasing rate, owing to initial axial force of the type stiffened with strut, is larger than that of other types and increased 130%.

CONFLICT OF INTEREST

The authors confirm that this article content has no conflict of interest.

ACKNOWLEDGEMENTS

This research is supported by grants from the Natural Science Foundation of China under Grant NO. 51308153, China Postdoctoral Science Foundation funded project NO. 2013M531020, Project HIT. NSRIF2014099 Supported by Natural Scientific Research Innovation Foundation in Harbin Institute of Technology.

REFERENCES

- [1] J. Schlaich, and H. Schober, "Glass-covered lightweight spatial structures," in Proc. IASS-ASCE Int. Symp. Atlanta 1994, pp. 1-27, 1994.
- [2] M. Saitoh, "Recent development of tension structures -aesthetics and technology of the strings-, current and emerging technologies of shell and spatial structures," in Proc. of the IASS Colloquium, Madrid, 1999, pp. 105-116.
- [3] M. Fujimoto, K. Imai, R. Kinoshita, and S. Kushima, "Buckling experiments of single layer two-way grid dome prestressed by PC bar under gravity load," in Proc. of IASS 40th Anniversary Congress, Madrid, 1999, B2.1-B2.10.
- [4] S. Kushima, M. Fujimoto, and K. Imai, "Experimental study on buckling behavior of single layer two-way grid dome with PC bars as diagonals", *J. Struct. Construct. Eng.*, vol. 603, pp. 85-92, 2006.
- [5] S. ushima, M. Fujimoto, and K. Imai , "Numerical results on buckling behaviors of single layer two-way grid dome with tension members", *J. Struct. Construct. Eng.*, vol. 617, pp. 121-128, 2007.
- [6] A. Takino, and K. Imai, "Development of Wooden Prefabricated Truss System," in Proc. of IASS Symp., 2005, pp. 675-680.
- [7] M. Fujimoto, K. Imai, T. Furukawa, and M. Kusunoki, "Experimental Study of Single Layer Two-way Grid Cylindrical Shell Roof Composed of KiT-wood Space Truss System with Round Timber," in Proc. of IASS-APCS Symp., 2003.
- [8] S. Kato, N. Yoshida, and S. Nakazawa, "Buckling strength of two-way single layer lattice domes stiffened by diagonal braces", *J. Struct. Construct. Eng.*, vol. 676, pp. 891-898, 2012.
- [9] J. Schlaich, and H. Schober, "Glass-covered lightweight spatial structures," in Proc. IASS-ASCE Int. Symp.1994, Atlanta, pp. 1-27, 1994.
- [10] M. Saitoh, "Recent development of tension structures -aesthetics and technology of the strings-, current and emerging technologies of shell and spatial structures," in Proc. of the IASS Colloquium, Madrid, pp. 105-118,1999.
- [11] M. Saito, and A. Okada, "Study on structural concept and characteristics of SKELSION", *Steel Construct. Eng.*, vol.1, no.3, pp. 57-66, 1994.
- [12] M. Kawaguchi, M. Abe, and I. Tatemichi, "Design Tests and Realization of Suspen-Dome System", *J. Int. Assoc. Shell Spatial Struct.*, pp. 179-192,1999.

Received: Ugr vgo dgt"44, 2014

Revised: Qevq dgt"52, 2014 "Ccepted: P qxgo dgt"23, 2014

© Zhonghao *et al.*; Licensee Bentham Open.

This is an open access article licensed under the terms of the Creative Commons Attribution Non-Commercial License (<http://creativecommons.org/licenses/by-nc/3.0/>) which permits unrestricted, non-commercial use, distribution and reproduction in any medium, provided the work is properly cited.